Applied Thermal Engineering 222 (2023) 119843

Contents lists available at ScienceDirect

Applied Thermal Engineering

journal homepage: www.elsevier.com/locate/ate

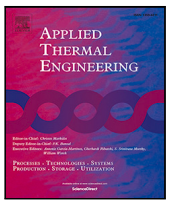

Research Paper

Field test of a geothermal thermoelectric generator without moving parts on the Hot Dry Rock field of Timanfaya National Park

Leyre Catalan *, Patricia Alegria, Miguel Araiz, David Astrain

Institute of Smart Cities, Public University of Navarre, 31006 Pamplona, Spain

ARTICLE INFO

Keywords:
Thermoelectric generator
Geothermal energy
HDR
Biphasic thermosyphon
Phase change
Heat pipe

ABSTRACT

Although in the last years thermoelectric generators have arisen as a solution to boost geothermal power generation, tests on field are still scarce. The vast majority of the available studies focus on computational simulations or laboratory experiments, mainly with active heat exchangers that require pumps or fans, and, consequently, present moving parts and auxiliary consumption. The present paper demonstrates for the first time the suitability of a geothermal thermoelectric generator (GTEG) with passive phase change heat exchangers, and therefore, without moving parts nor auxiliary consumption, on the shallow Hot Dry Rock (HDR) field of Timanfaya National Park (Canary Islands, Spain), where 173 °C air anomalies can be found. The device has been in operation without maintenance for 2 years now, producing more than 520 kWh of energy. In terms of power generation, since the installed device is in turn composed of two prototypes with 10 and 6 thermoelectric modules, it has been confirmed that installing more modules leads to a lower generation per module, although total generation can be higher. In fact, the prototype with 10 thermoelectric modules generated a maximum of 20.9 W (2.09 W per module) with a temperature difference between sources of 158 °C, while the prototype with 6 thermoelectric modules obtained 16.67 W (2.78 W per module) under the same conditions. These results open the door for a large-scale exploitation thanks to the intrinsic advantages of modularity, reliability, robustness, and minimal environmental impact of the developed device.

1. Introduction

Despite the efforts made in the last years, fossil fuels still remain dominant in the global energy scenario, accounting for 78.5% of global energy demand and being responsible of three-quarters of global CO_2 emissions [1]. Therefore, a structural shift in the global energy system is increasingly urgent [1], trying to stop emissions that contribute to climate change and leading to energy independent countries. For this purpose, it is necessary to take into account all renewable sources, since a combination of them will permit achieving the desired objectives.

The present paper focuses on one of the largest renewable sources, geothermal energy, which, in comparison with other sources, presents the advantage of being independent of weather, thus providing stability and a high potential. Furthermore, it can be used for heating-cooling applications as well as for electricity generation. Nevertheless, its contribution to the global energy scenario is minimal, specially in electricity generation, with less than 0.4% of the global demand [2], mainly due to the high initial investment, the long payback and construction time, as well as the difficulties assessing the resource and modularizing [3].

In order to speed up the growth of geothermal power, thermoelectric generators have been identified as one of the technologies that "may make breakthrough" [3]. Thermoelectric generators (TEGs) are solid-state devices whereby heat is directly converted into electricity, and that present the advantage of being modular, compact, and permitting a noiseless generation without moving parts, which minimizes maintenance. The latter characteristics are intrinsic to the thermoelectric modules, the core of TEGs in which the transformation is held due to the Seebeck effect. Nonetheless, the whole generator would maintain such advantages or not depending on the heat exchangers that are used in order to maximize the temperature difference between the sides of the thermoelectric modules, as their efficiency mainly depends on it, with higher efficiencies with higher temperature differences. Thus, it is not only important to have low thermal resistances on the heat exchangers, as a 10% reduction on the thermal resistance leads to an 8% higher generation [4], but also to take into account that those heat exchangers with auxiliary equipment such as fans or pumps include moving parts, avoiding the mentioned benefits, and also have associated an extra power consumption that reduces net generation.

* Corresponding author.
E-mail address: leyre.catalan@unavarra.es (L. Catalan).

https://doi.org/10.1016/j.applthermaleng.2022.119843
Received 30 September 2022; Received in revised form 1 December 2022; Accepted 7 December 2022
Available online 16 December 2022

Nomenclature

Variables

$\dot{Q}$	Heat flux (W)
η	Efficiency (%)
E	Energy (kW h)
m	Number of thermoelectric modules
P	Electric Power (W)
R	Thermal resistance (K/W)
T	Temperature (K)
t	Time (h)

Subscripts and Superscripts

amb	Ambient
C	Cold side
CHE	Cold side heat exchanger
g	Geothermal air
H	Hot side
HHE	Hot side heat exchanger
TEM	Thermoelectric module
$total$	Total

Abbreviations

CCTEG	Concentric Cylindrical Thermoelectric Generator
GTEG	Geothermal Thermoelectric Generator
HDR	Hot Dry Rock
TEG	Thermoelectric Generator
TEM	Thermoelectric module

In the literature, most of the proposed geothermal thermoelectric generators (GTEGs) use heat exchangers with a circulating fluid, which, although present moving parts and auxiliary consumption, recall to traditional geothermal power systems based on Rankine cycles. Hence, the circulating fluid is pumped into the ground, absorbing geothermal heat and transporting it to the thermoelectric modules, which will transform part of this heat into electricity, releasing the rest to the environment, normally with another heat exchanger with a pumped circulating fluid. With such configuration, Niu et al. built a device capable of generating 146.5 W with a temperature difference between sources of 120 °C and 56 thermoelectric modules (2.62 W per module) [5]. Ahiska and Mamur also demonstrated the feasibility of this configuration with a prototype capable of producing 41.6 W under a 100 °C gradient with 20 modules (2.08 W per module) [6]. On their behalf, Suter et al. preferred to perform a computational analysis, and optimized a 1 kW thermoelectric stack by simulating different operating parameters and geometries [7].

More recently, some authors have focused on the improvement of the hot side heat exchanger in order to extract as much geothermal heat as possible. This is the case of Ding et al. who believe in the advantages of thermoelectric generators for geothermal power generation (packaging, lack of moving parts, direct heat to electrical conversion, and zero-emission), and that designed segmented annular concentric cylindrical thermoelectric generators (CCTEGs) and evaluated them with a mathematical model, leading to a generation of 136 kW under a temperature difference between sources of 130 °C with a 500 m long CCTEG system with 100 segmented thermoelectric generators and 1500 × 470 P-N semiconductors in each generator [8]. Liu et al. were also convinced that segmented concentric cylindrical thermoelectric generators are the best configuration. In their case, they evaluated their suitability in oil and gas wells, following the studies of Wang et al. [9,10], in order to supply power to the downhole sensors and control tools. With a mathematical model, they estimated a generation of 800 W with a CCTEG system with a total length of 200 m composed of 40 segmented thermoelectric generators with 1500 × 70 P-N elements per generator [11].

Nonetheless, although the configuration with heat exchangers with a circulating fluid is the most common one, some authors, such as Xie et al. believe that these conventional geothermal exploitation technologies with water extraction bring on many issues such as high operation cost, low electricity generation efficiency, and huge environmental impact [12]. Therefore, they propose the use of heat pipes or biphasic thermosyphons for geothermal heat extraction. This type of heat exchangers are based on phase change, permit transporting great amounts of heat almost isothermally, and do not require auxiliary equipment since fluid moves thanks to density differences, gravity, and, in the case of heat pipes, wick materials [13]. Deng et al. agree that these heat exchangers are the most suitable ones to absorb geothermal heat [14]. In their case, they proposed two-phase thermosyphons to extract heat from coalfields and reduce subsurface fires and their ecological disasters while generating electricity with a TEG, estimating a generation of 960 W per hole. A similar configuration of TEG, with a heat pipe as hot side heat exchanger and circulating water in the cold side, was proposed by Zhao et al. [15] for geothermal power generation. They delved into their operation at the laboratory, making the device work under different conditions and with different number of thermoelectric modules. In their study, they found that, although the maximum efficiency of a single module is achieved with a generator composed of only one thermoelectric module, in terms of total generation it is better to include more modules until a maximum is reached. With their specific configuration, the best alternative consisted of four thermoelectric modules, which led to 10.85 W in total.

The first geothermal thermoelectric generator (GTEG) that included phase change heat exchangers at both sides of the thermoelectric modules was developed by Catalan et al. achieving a completely passive device, without moving parts nor auxiliary consumption; thus extrapolating the benefits of thermoelectricity to the whole generator [16]. In fact, they demonstrated at the laboratory that this configuration leads to a 54% higher generation than with fin dissipaters at the cold side: 3.29 W per module with a temperature difference between sources of 180 °C. Afterwards, they delved into the study of such configuration by means of a computational model validated thanks to the previous experimental data [17]. In this study, they reached the same conclusion as Zhao et al. [15] regarding the influence of the number of thermoelectric modules, determining that there is an optimal number of thermoelectric modules per device due to the weight of each thermal resistance. Based on this model, they designed and built two prototypes and tested them at the laboratory, as gathered by Alegria et al. [18]. Under a thermal gradient between sources of 160 °C, the first prototype was able to generate 17 W with 10 thermoelectric modules, while the second one led to 19 W with 6 thermoelectric modules, demonstrating in practice that with less modules, the generation per module increases and so does efficiency.

The present paper continues analyzing the behavior of the former GTEG [18], but it goes a step further, studying it on field. As has been observed, the tendency in the literature is to make computational studies or laboratory experiments. However, in order to boost the development of GTEGs and make them finally a reality, it is necessary to know their behavior on real geothermal fields. In the literature, few examples of low-power generators oriented to sensors can be found [19–21]. Nonetheless, Li et al. are the only ones that have developed and tested a large-scale generation device on field. Focused on making a modular device, after several investigations [22–25] they ended up designing and building a five-layer thermoelectric generator with 90 thermoelectric modules that can be installed with modularized units. In the laboratory, they were able to generate an electric power of 45.7 W with a temperature difference of 72.2 °C between the cold and hot sides (0.51 W per module). Afterwards, they tested the device during two days at Bottle Rock (The Geysers, California, USA) after

an upgrade to a six-layer device [26]. The whole six-layer TEG could generate on field about 500 W electricity with a temperature difference of approximately 152 °C between the hot and cold fluid manifolds (3.9 W per module). Nevertheless, in order to achieve such values, heat exchangers with a circulating fluid and, consequently, moving parts and auxiliary consumption, were used.

Thanks to the use of phase change heat exchangers, the present paper supposes the first large-scale generation device without moving parts that it is installed and analyzed on field. In particular, this research studies the effect of the number of thermoelectric modules and the environmental conditions on the temperature distribution, power generation, efficiency, and energy production of a GTEG installed at Timanfaya National Park (Lanzarote, Canary Islands, Spain), one of the most significant Hot Dry Rock (HDR) fields in the world, with anomalies where geothermal gases ascend to the surface with a temperature between 150 and 500 °C [27]. The device was installed on field in August 2020, which implies more than two years of continuous operation, a sufficiently long time period to deeply know the behavior of the developed GTEG for the sake of a future large-scale installation thanks to the scalability of the design and its minimal environmental impact.

2. Operation and installation of the geothermal thermoelectric generator (GTEG)

Although the device that has been experimented on field in this paper is the same than the one developed by Alegria et al. [18], since the anomalies available at Timanfaya National Park (Lanzarote, Canary Islands, Spain) are of gaseous nature (hot gases emerge from the boreholes), it is necessary to introduce slight modifications to the design in order to improve heat transfer with the geothermal gases. Thus, the extruded aluminum pattern with 31 fins 17 mm high and 2 mm thick detailed in Fig. 1 has been added along the lowest 1.5 m of the hot side heat exchangers, where rope heaters provided heat at the laboratory. These heat exchangers are cylindrical biphasic thermosyphons made of copper with a diameter of 41.27 mm, a thickness of 1.25 mm, and water as working fluid (0.5 m high). As depicted in the figure, the inferior 2 m are inserted in the borehole, while the overground length depends on the specific prototype. Thus, Prototype A, with 10 thermoelectric modules (5 levels), stands 1 m above ground, while Prototype B, with 6 thermoelectric modules (3 levels), presents an overground height of 0.85 m.

Geothermal heat causes the vaporization of the water inside each hot side heat exchanger, which ascends to the upper part of the tubes. In this part, the heat is released to the thermoelectric modules, condensing and returning to the inferior part thanks to gravity. Nonetheless, since the hot side heat exchanger is round and the thermoelectric modules are planar, a 60 mm^2 squared copper block 40 mm high and graphite sheets have been added as detailed in Fig. 2 in order to ensure a good thermal contact.

The used thermoelectric modules are the commercial Marlow TG12-8LS, with 127 Bismuth-Telluride thermocouples and a maximum operating temperature of 230 °C. These modules transform part of the heat directly into electricity, releasing the rest to the environment. For this purpose, again heat exchangers based on phase change have been used, as it was demonstrated by Catalan et al. that are the most suitable ones for this application [16]. As depicted in Figs. 1 and 2, each thermoelectric module counts with its own cold side heat exchanger, which is composed of four copper sintered heat pipes with a diameter of 8 mm and a length of 500 mm inserted in an aluminum fin dissipater with a 14.5 mm thick base and fifteen 40 × 1.5 mm^2 corrugated fins. With the objective of improving heat dissipation, 104 × 27.5 × 0.3 mm^3 aluminum fins have also been added to the heat pipes with a separation of 5 mm.

The operation of this GTEG has also been represented in Fig. 3 by means of the schematics of thermal resistances. Thus, each prototype

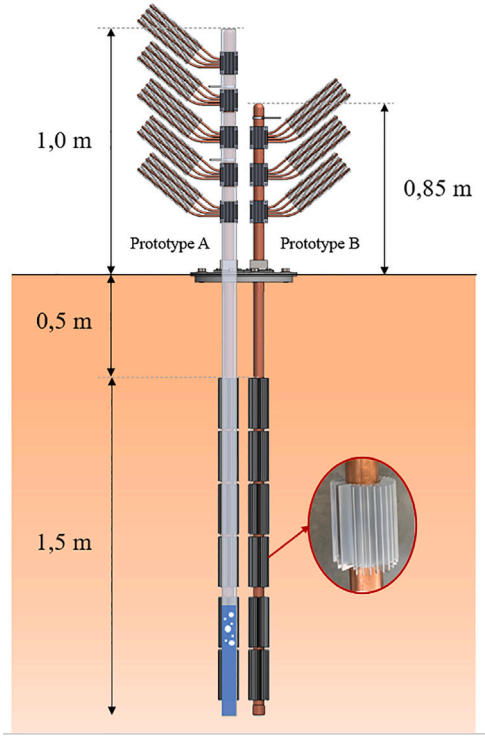

Fig. 1. 3D representation of the installed geothermal thermoelectric generator (GTEG), detailing its dimensions, the operation of the hot side heat exchangers, and the extruded aluminum fins.

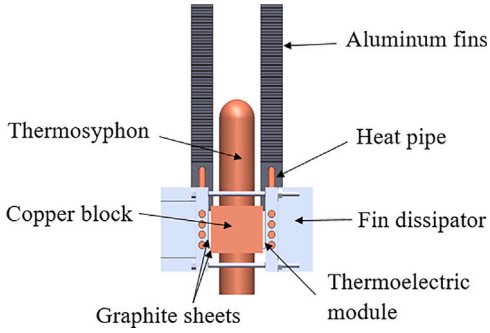

Fig. 2. Detail of the assembly between the heat exchangers and the thermoelectric modules.

has a unique hot side heat exchanger, depicted by R_{HHE}, that absorbs geothermal heat $\dot{Q}_H$. This heat is transferred to the thermoelectric modules, each of which has its own cold side heat exchanger, as represented by the branches composed by the thermal resistances R_{TEM} and R_{CHE}. Part of the heat absorbed by each thermoelectric module ($\dot{Q}_H$ divided by the number of modules m) is transformed into electrical energy P_{TEM_i}, releasing the rest ($\dot{Q}_C$) to the environment, as indicated by Eq. (1). The total power generated by the prototype P_{total} will be obtained by the addition of the individual power of each module (Eq. (2)), while its efficiency η derives from Eq. (3).

$$P_{TEM_i} = \frac{\dot{Q}_H}{m} - \dot{Q}_C \tag{1}$$

$$P_{total} = \sum_{i=1}^{m} P_{TEM_i} \tag{2}$$

$$\eta = \frac{P_{total}}{\dot{Q}_H} \tag{3}$$

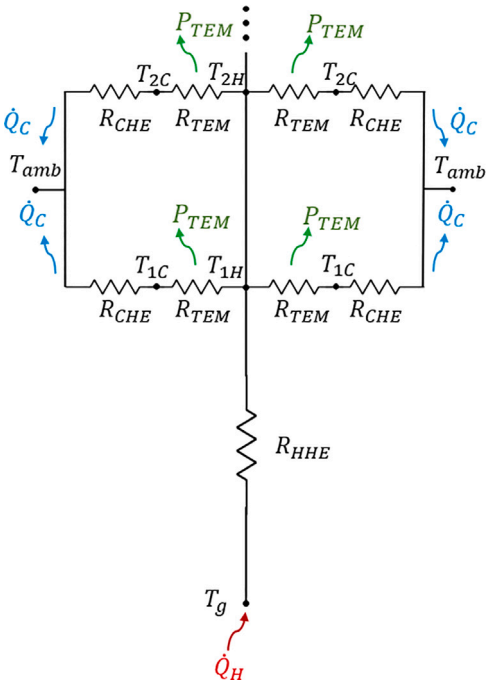

Fig. 3. Schematics of the operation of the developed prototypes with thermal resistances.

The heat flux that is extracted from the geothermal gases $\dot{Q}_H$ corresponds, in turn, with Eq. (4), which is obtained dividing the temperature difference between the geothermal air T_g and the hot side of the thermoelectric modules T_H by the thermal resistance of the hot side heat exchanger R_{HHE}. This heat flux can also be approximated as the temperature difference between the ground T_g and the environment T_{amb} divided by the total thermal resistance of the prototype R_{total}, whose expression is detailed in Eq. (5) taking into account that there is a common hot side heat exchanger and several parallel branches with the thermoelectric modules. Similarly, the heat flux that is released by each thermoelectric module follows the expression depicted in Eq. (6), with the temperature difference between the cold side of the thermoelectric modules T_C and the environment T_{amb}, divided by the thermal resistance of the cold side heat exchanger R_{CHE}.

$$\dot{Q}_H = \frac{T_g - T_H}{R_{HHE}} = \frac{T_g - T_{amb}}{R_{total}} \tag{4}$$

$$R_{total} = R_{HHE} + \frac{R_{TEM} + R_{CHE}}{m} \tag{5}$$

$$\dot{Q}_C = \frac{T_C - T_{amb}}{R_{CHE}} \tag{6}$$

If the thermal resistances of the heat exchangers are reduced, the temperatures of the hot and cold sides of the thermoelectric modules will resemble better the ground and ambient temperatures respectively. Thus, with a greater temperature difference between the sides of the thermoelectric modules, their efficiency will increase and more power will be generated. Nonetheless, it is also necessary to take into account that the generated power is also influenced by the number of thermoelectric modules installed [15,17]. Hence, with more thermoelectric modules m, the total thermal resistance of the prototypes R_{total} is reduced. According to Eq. (4), this causes an increase in the heat flux that is absorbed from the geothermal field $\dot{Q}_H$. Since the thermal resistance of the hot side heat exchanger remains constant with the heat flux [18], this means that the temperature of the hot side of the thermoelectric modules will diminish. Therefore, the more thermoelectric modules, the lower the temperature difference between the sides of the modules, reducing generation. In fact, as it was demonstrated by Catalán et al. and also addressed by Zhao et al. [15], there is an optimal number of thermoelectric modules when total generation reaches its maximum [17]. Since the present paper studies a generator composed of two prototypes, one with 10 thermoelectric modules (Prototype A) and other with only 6 (Prototype B), this effect will be analyzed in depth in the next section thanks to the results obtained on field.

Fig. 4. Location of the GTEG installed at Timanfaya National Park, in the area of *Casa de los Camelleros*.

2.1. Installation of the GTEG on field

The device described above was installed at Timanfaya National Park, in the area of *Casa de los Camelleros* (Fig. 4), on 27th August 2020, which supposes two complete years at the moment of writing the present manuscript. Specifically, the device was installed in an existing borehole with a diameter of 305 mm and a depth of 31 m, where geothermal gases go out with a temperature of around 170 °C and an approximate velocity of 6 m/s.

In order to avoid the hot geothermal gases to affect the operation of the cold side of the generator, a deflector was added to the base of the borehole as depicted in Figs. 5 and 6. For this purpose, it is also important that the device has a proper orientation regarding the predominant wind direction. Therefore, the device was installed facing N-NE, so that the geothermal gases are diverted away from the generator, at the same time that the operation of the cold side heat exchangers is optimized. To ensure that heat is only evacuated through these cold side heat exchangers, the outer parts of the hot side heat exchangers where there are no thermoelectric modules were insulated with rock-wool and protected with aluminum tape.

The device also included a monitoring system in order to register its behavior. On the one hand, thermocouples were installed in order to measure the temperature of the geothermal gases T_g, the temperature of the hot T_H and cold T_C sides of the thermoelectric modules installed in the first and last levels of each prototype, as well the ambient temperature T_{amb}. On the other hand, the power generation of each level, where two thermoelectric modules are connected in series to the optimal electrical resistance of 6.4 Ω [18], was also measured. In both cases, an Arduino Mega was used for the measurements every 30 s, with type K thermocouples connected to MAX31855 for temperature measurements [28], and INA219 for the power generation ones [29]. Finally, a meteorological station was also installed in order to measure the wind velocity and its direction.

3. Results and discussion

Once the device and its installation on field have been described, this section deals with the analysis of the results monitored during

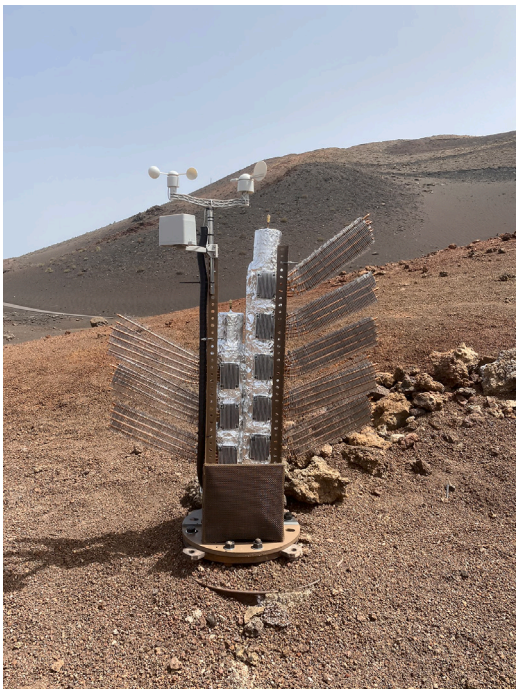

Fig. 5. Complete device installed at Timanfaya National Park, with Prototype A on the right, Prototype B on the left, and the deflector on the borehole.

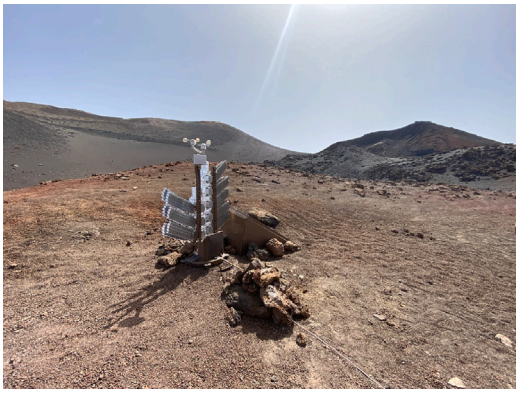

Fig. 6. Panoramic view of the complete device installed at Timanfaya National Park.

the last two years, detailing its operation first and making a global analysis afterwards. During this time, it is important to highlight that no maintenance has been performed thanks to the robustness of the passive heat exchangers that have been installed, with no moving parts nor auxiliary consumption.

Firstly, Fig. 7 depicts the temperature distribution of both prototypes on a typical week in April with predominant N-NE wind, showing the temperature of the geothermal gases T_g, the temperature of the hot T_H and cold T_C sides of the thermoelectric modules located at the lowest and highest levels of each prototype (1 and 5 in case of Prototype A, and 1 and 3 in case of Prototype B), as well as the ambient temperature T_{amb}. As can be observed, the geothermal gases always ascend with a constant temperature of around 173 °C, while ambient temperature suffers the greatest variations, oscillating during night and day between 18 and 35 °C in the selected week. The desirable temperature difference in the thermoelectric modules is the one between the former temperatures. However, in reality, the sides of the modules present a lower gradient, which is in turn affected by the thermal resistances of the heat exchangers. Thus, it can be seen

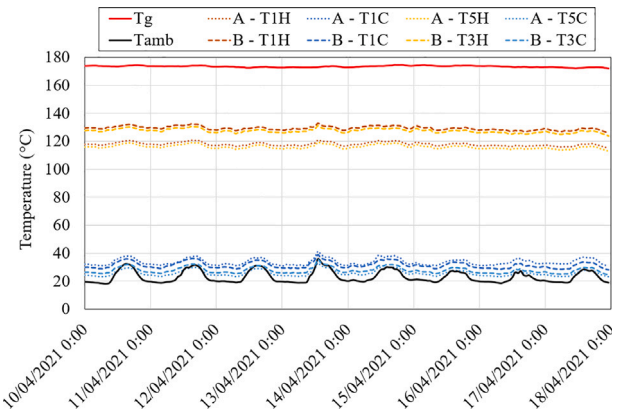

Fig. 7. Temperature distribution of the geothermal gases T_g, the hot T_H and cold T_C sides of the thermoelectric modules located at the lowest and highest levels of each prototype, and the ambient T_{amb} during one week in April 2021.

that the temperatures of the cold sides of the thermoelectric modules are very close to the ambient temperature, being practically similar during the day and with a difference of less than 10 °C during the night independently of the prototype. Regarding the levels, both prototypes present the same behavior, with slightly lower temperatures at the highest levels due to the greater distance to the geothermal gases.

In contrast, there exists a greater temperature loss between the geothermal gases and the hot side of the thermoelectric modules that is due to the low convection coefficients between the geothermal gases and the hot side heat exchangers, which still have a great weight in the thermal resistance despite the addition of fins. More specifically, in Prototype B the temperature difference is of approximately 45 °C, while in Prototype A the loss ascends to 56 °C. This 11 °C difference is related with the number of thermoelectric modules installed, with 6 thermoelectric modules (3 levels) in Prototype B and 10 modules (5 levels) in Prototype A. As has been explained before and according to Eq. (5), with a higher number of thermoelectric modules m, the total resistance of the prototype is reduced. Therefore, given a certain temperature difference between the geothermal gases and the ambient, the heat flux extracted from the geothermal field increases as deduced from Eq. (4). Consequently, since both prototypes have the same hot side heat exchanger, whose thermal resistance does not vary with the heat flux [18], according to the same equation, with a higher number of thermoelectric modules, the temperature difference between the geothermal gases and the hot side of the thermoelectric modules increases, leading to a lower T_H with more thermoelectric modules. This in turn provokes a lower temperature difference between the sides of the thermoelectric modules, which diminishes generation per module, as can be observed in Fig. 8 during the same period of time. Hence, while each level of Prototype B generates an average power of 5.1 W, in Prototype A each level produces 4.1 W, with exception of level 5 with 60% of the power, which seems to be due to a poor contact or to a failure in the modules of this level since the temperature difference between their sides was similar. Nonetheless, despite the lower generation per module, total generation of the prototype can be higher, as it was computationally demonstrated by Catalan et al. [17] and it is experimentally observed in reality. Thus, Prototype A presents a higher generation, with an average of 18.9 W in the selected week, 23.5% higher than Prototype B, with an average of 15.3 W. It is important to highlight that all this generation is net, due to the passive nature of the used heat exchangers.

If instead of analyzing a unique week, the whole two years are taken into consideration, the former statement remains true regardless the external conditions. This can be observed in Fig. 9, which represents the average power generation of each prototype every two hours with respect to the temperature difference between the geothermal gases

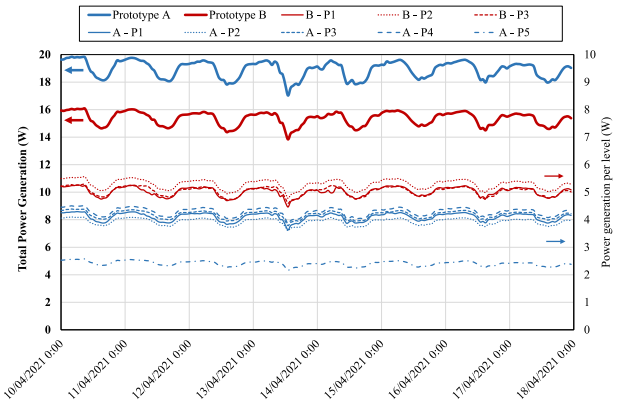

Fig. 8. Power generation per level of Prototype A, with 5 levels, and Prototype B, with 3 levels (thin lines — right axis), as well as total generation of each prototype (thick lines — left axis) during one week in April 2021..

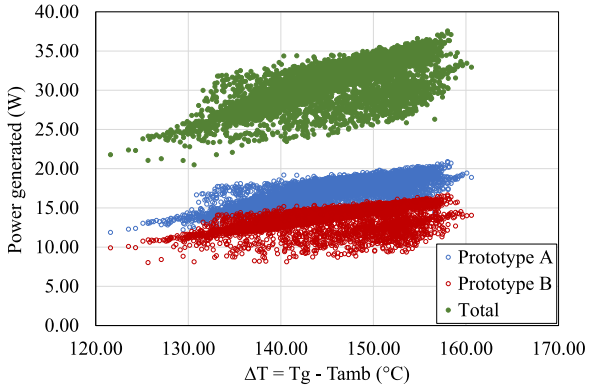

Fig. 9. Average power generation of each prototype every two hours with respect to the temperature difference between the geothermal gases T_g and the ambient T_{amb}.

T_g and the ambient T_{amb}, with Prototype A in blue, Prototype B in red, and the total generation of the device (sum of Prototypes A and B) in green. In general, power generation follows a linear tendency with respect the temperature difference between the heat sources, with a slightly deeper slope in the case of Prototype A due to the higher number of thermoelectric modules. Alegria et al. also obtained this linear tendency at the laboratory, when supplying heat directly to the external part of the hot side heat exchanger by means of rope heaters [18]. However, they obtained that Prototype B generated more at all conditions (not comparable with these ones). The present paper studies on field the same prototypes, but before their installation, they were reassembled, which explains the results obtained now, more in concordance with the study of Catalan et al. that stated that for these conditions, the optimal number of modules should be beyond 10 [17]. Therefore, with more thermoelectric modules, total generation could be increased, although this will increase the total height of the device and, consequently, its visual impact, something of utmost importance for Timanfaya National Park, who recommends a maximum exterior height of 1 m, which corresponds with Prototype A.

In Fig. 9 it can also be observed that there are some points that do not follow the linear tendency. This is due to the fact that the exterior conditions are not always the same for a similar temperature difference between the sources, specially regarding the intensity and direction of the wind. For instance, with a temperature difference between 156 and 158 °C, both a generation of 26.31 W and the maximum generation of 37.57 W (20.90 W of Prototype A, and 16.67 W of Prototype B) have been obtained. In order to analyze more in depth this fact, Fig. 10 represents the temporal series of the total generation of both prototypes, the

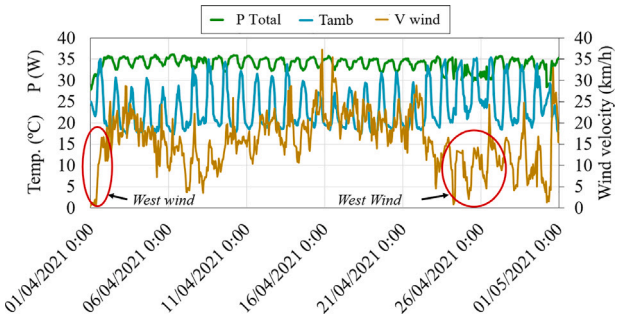

Fig. 10. Total power generation of both prototypes, ambient temperature and wind velocity during April 2021.

ambient temperature - in the left axis - and the wind velocity - in the right axis - measured every 30 s during April, which represents the average conditions available throughout the year. The temperature of the geothermal gases has not been represented since it presents a constant value of 173 °C.

As can be observed, total generation is firstly conditioned by ambient temperature. Thus, during the day, ambient temperature rises, leading to a lower generation since the temperature difference between the sides of the thermoelectric modules decreases. In contrast, during the night, with lower ambient temperatures, this temperature gradient increases, and so does total generation. In this month, total generation normally oscillates between 32.5 and 35.5 W. Nevertheless, there are some periods of time in which total generation diminishes. This reduction occurs when the wind velocity decreases, which worsens the heat dissipation of the cold side heat exchangers due to lower convection coefficients. Moreover, with lower wind velocities, the hot geothermal gases are not properly evacuated, ascending due to lower densities and affecting the behavior of the cold side heat exchangers. An example of power reduction can be observed the dawn of 30th April 2022, when wind velocity decreased from 13 to 1.3 km/h, causing a 17% reduction in total generation, from 34.3 W to 28.5 W. This effect also occurs when the wind comes from the W-SW direction, as indicated by the red circles in Fig. 10, which causes that the hot geothermal gases are impulsed directly to the prototypes. Nonetheless, according to the wind rose of Lanzarote, most of the time there is a considerable wind with predominant N-NE direction [30], which leads to scant periods of diminished generation, as corroborated in Fig. 11, where the generation of each prototype during the two years of study is represented.

Apart from the temperature distribution and power generation, it also results interesting to calculate the efficiency of each prototype. Thus, for the average ambient temperature and wind velocity of Lanzarote (21.9 °C and 22 km/h), the average efficiency η of each prototype has been calculated based on the average temperature difference between the sides of the thermoelectric modules and the datasheet provided by Marlow [31]. As can be observed in Table 1, the lower temperature difference between the sides of the thermoelectric modules of Prototype A leads to a lower generation per thermoelectric module (P/TEM) despite the higher generation of the whole prototype, which causes a lower efficiency of Prototype A: 3.26% versus 3.57% of Prototype B. Reiterating in previous explanations, this is due to the fact that with more thermoelectric modules, the total thermal resistance diminishes, leading to a bigger absorption of geothermal heat, but provoking a lower hot side temperature in the thermoelectric modules. This is corroborated in the table, where the heat flux absorbed from the geothermal field has been estimated by using the definition of efficiency (Eq. (3)). Thanks to this estimation, and since the average temperatures of the geothermal gases (173 °C) and the hot side of the thermoelectric modules are known (115.8 °C in Prototype A and 127.6 °C in Prototype B), it has been possible to calculate the thermal resistance of the hot side heat exchangers following Eq. (4), obtaining an average value

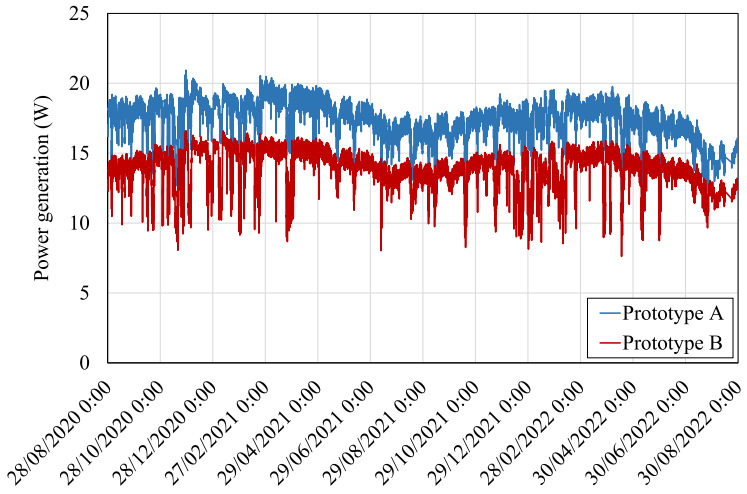

Fig. 11. Average generation of each prototype every two hours from August 2020 to August 2022.

Table 1
Estimation of the efficiency η, the heat flux absorbed from the geothermal field $\dot{Q}_H$, and the thermal resistances of the heat exchangers R_{HHE} and R_{CHE}, based on the temperature difference between the sides of the thermoelectric modules ΔT_{H-C} and their generation P with the average ambient conditions of Lanzarote.

Prototype	ΔT_{H-C} (°C)	P (W)	P/TEM (W)	η (%)	$\dot{Q}_H$ (W)	R_{HHE} (K/W)	R_{CHE} (K/W)
A	86.27	18.84	1.88	3.26	577.67	0.099	0.123
B	98.23	15.29	2.55	3.57	428.47	0.106	0.092

of 0.1025 K/W. For the calculation of the average thermal resistance of the cold side heat exchangers, firstly the heat dissipated by each thermoelectric module has been estimated with Eq. (1). Next, thanks to Eq. (6) and the average temperature of the cold sides of the thermoelectric modules (28.8 °C in Prototype A and 28.2 °C in Prototype B), the average thermal resistance of the each cold side heat exchanger has been obtained, leading to an average of 0.1075 K/W. Although the thermal resistances of both the hot and the cold heat exchangers are quite similar, with considerably low values taking into account their passive nature, it is important to highlight that the calculated results consider the thermal resistance of each individual heat exchanger. The prototypes share a common hot side heat exchanger, while each thermoelectric module has its own cold side heat exchange. Therefore, in the total thermal resistance of the device, the resistances of both the modules and the cold side heat exchangers are divided by the number of thermoelectric modules (Eq. (5)), and so does the absorbed heat $\dot{Q}_H$, which causes a lower temperature difference between the cold side and the ambient in comparison with the gradient between the geothermal gases and the hot side of the thermoelectric modules, despite the similar values of the thermal resistances.

Finally, in order to finish with a broad view of the generation of the device during its first two years, the energy generated by each prototype has been calculated. For this purpose, taking into account the hourly average power measurement of both prototypes P_{total} and the time range t (1 h), energy E has been calculated as $E = P_{total} \cdot t$. Fig. 12 represents the values obtained monthly, from September 2020 to August 2022. As can be observed, the total generated energy oscillates between 20 and 25 kWh, remaining considerably constant if compared with other renewable sources thanks to the stability of geothermal temperature. The variations are mainly due to the external ambient conditions. Thus, although winter months tend to have the lowest temperature, energy generation is higher in spring and autumn because of the stronger wind conditions combined with moderate temperatures. In fact, the maximum energy production corresponds to March 2021, with almost 25 kWh, since the fastest wind speeds were registered in this period. In total, during the two years considered in the present paper, more than 520 kWh have been generated, which supposes

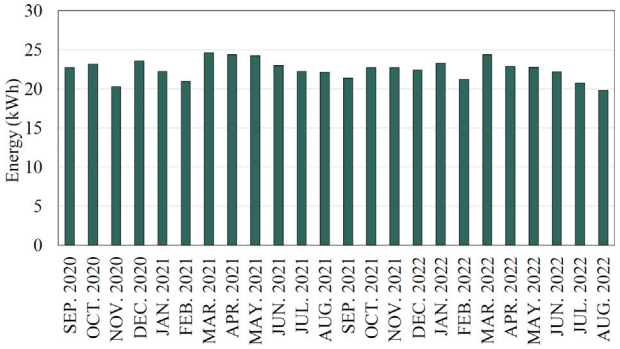

Fig. 12. Total energy production of the two prototypes during two years of operation.

270.25 kWh per year and, taking into account the occupied surface, 180.16 kWh/m^2. Thanks to the modularity of the proposed design and its minimal environmental impact, these results open the door for a larger scale exploitation at Timanfaya National Park, which would permit reducing the dependency of fossil fuels while guaranteeing a base-load power supply. Moreover, since it has been demonstrated during these two years that maintenance is not necessary due to the absence of moving parts, costs are reduced, entailing a promising and very attractive alternative.

4. Conclusions

In conclusion, the present paper supposes the first large-scale geothermal thermoelectric generator (GTEG) without moving parts that has been installed and analyzed on field. In the literature, most of the existing studies focus on computational simulations or laboratory experiments, mainly with active heat exchangers that require pumps or fans, and, consequently, have moving parts and auxiliary consumption. Nonetheless, this work has demonstrated the suitability and robustness of a GTEG with passive phase change heat exchangers (without moving

parts nor auxiliary consumption) that has been in operation without maintenance for more than 2 years in the shallow Hot Dry Rock (HDR) field of Timanfaya National Park (Lanzarote, Canary Islands, Spain), where geothermal gases ascend at an approximate temperature of 173 °C.

The installed device is composed of two prototypes, with the only difference of having 10 or 6 thermoelectric modules, thus permitting the analysis of the effect of the number of thermoelectric modules besides the environmental conditions. Hence, it has been confirmed in practice that a higher number of thermoelectric modules increases total generation, although generation per module is reduced. Thus, the prototype with 10 thermoelectric modules has produced a maximum power of 20.90 W (2.09 W per module) with a temperature difference between sources of 158 °C, while the one with 6 modules obtained a maximum of 16.67 (2.78 W per module). This is due to the fact that each prototype shares a common hot side heat exchanger with all the thermoelectric modules, each of which has its own cold side heat exchanger. Therefore, with more thermoelectric modules, the total thermal resistance of the prototype is reduced, absorbing more geothermal heat, but causing a reduction in the temperature of the hot side of the thermoelectric modules that diminishes its thermal gradient and therefore generation. This is also reflected in the efficiency, with an efficiency with average conditions of 3.26% with 10 thermoelectric modules and of 3.57% in the case of having 6.

Besides the effect of the number of thermoelectric modules, the influence of the environmental conditions has also been analyzed, obtaining a practically linear dependency between power generation and the temperature difference between the geothermal gases and the ambient, which is slightly reduced in case of unfavorable wind conditions. Nonetheless, despite the variations with the meteorology, the monthly energy production is quite stable, with values between 20 and 25 kWh that have permitted obtaining more than 520 kWh in two years. Therefore, these results expose the suitability of the developed prototypes and open the door for a larger scale exploitation at Timanfaya National Park thanks to the modularity, reliability, robustness, and minimal environmental impact of the developed device.

Declaration of competing interest

The authors declare that they have no known competing financial interests or personal relationships that could have appeared to influence the work reported in this paper.

Data availability

Data will be made available on request.

Acknowledgments

The authors would like to acknowledge the support of the Spanish State Research Agency and FEDER-UE under the grants PID2021-124014OB-I00 and TED2021-129359B-I00, as well as the collaboration of Timanfaya National Park in the installation of the prototypes. Open access funding provided by Universidad Pública de Navarra.

References

[1] REN21, Renewables 2022 Global Status Report, 2022.
[2] REN21, Renewables 2021 Global Status Report, 2021.
[3] K. Li, H. Bian, C. Liu, D. Zhang, Comparison of geothermal with solar and wind power generation systems, Renew. Sustain. Energy Rev. 42 (2015) 1464–1474, http://dx.doi.org/10.1016/j.rser.2014.10.049.
[4] D. Astrain, J.G. Vián, A. Martínez, A. Rodríguez, Study of the influence of heat exchangers' thermal resistances on a thermoelectric generation system, Energy 3 (2010) 602–610, http://dx.doi.org/10.1016/j.energy.2009.10.031.
[5] X. Niu, J. Yu, S. Wang, Experimental study on low-temperature waste heat thermoelectric generator, J. Power Sources 188 (2009) 621–626, http://dx.doi.org/10.1016/j.jpowsour.2008.12.067.
[6] R. Ahiska, H. Mamur, Design and implementation of a new portable thermoelectric generator for low geothermal temperatures, IET Renew. Power Gener. 7 (2013) 700–706, http://dx.doi.org/10.1049/iet-rpg.2012.0320.
[7] C. Suter, Z.R. Jovanovic, A. Steinfeld, A 1kWe thermoelectric stack for geothermal power generation - Modeling and geometrical optimization, Appl. Energy 99 (2012) 379–385, http://dx.doi.org/10.1016/j.apenergy.2012.05.033.
[8] T. Ding, J. Liu, K. Shi, S. Hu, H. Yang, Theoretical study on geothermal power generation using thermoelectric technology: a potential way to develop geothermal energy, Int. J. Green Energy 18 (2021) 297–307, http://dx.doi.org/10.1080/15435075.2020.1854271.
[9] K. Wang, J. Liu, X. Wu, Downhole geothermal power generation in oil and gas wells, Geothermics 76 (2018) 141–148, http://dx.doi.org/10.1016/j.geothermics.2018.07.005.
[10] K. Wang, X. Wu, Downhole thermoelectric generation in unconventional horizontal wells, Fuel 254 (2019) 115530, http://dx.doi.org/10.1016/j.fuel.2019.05.113.
[11] J. Liu, Z. Wang, K. Shi, Y. Li, L. Liu, X. Wu, Analysis and modeling of thermoelectric power generation in oil wells: A potential power supply for downhole instruments using in-situ geothermal energy, Renew. Energy 150 (2020) 561–569, http://dx.doi.org/10.1016/j.renene.2019.12.120.
[12] H. Xie, J. Wang, J. Liao, X. Long, C. Li, B. Li, J. Ma, A novel in-situ power generator system for geothermal resources without fluid extraction, in: 55th U.S. Rock Mechanics - Geomechanics Symposium 2021, 2021.
[13] H. Shabgard, M.J. Allen, N. Sharifi, S.P. Benn, A. Faghri, T.L. Bergman, Heat pipe heat exchangers and heat sinks: Opportunities, challenges, applications, analysis, and state of the art, Int. J. Heat Mass Transfer 89 (2015) 138–158, http://dx.doi.org/10.1016/j.ijheatmasstransfer.2015.05.020.
[14] J. Deng, F. Zhou, B. Shi, J.L. Torero, H. Qi, P. Liu, S. Ge, Z. Wang, C. Chen, Waste heat recovery, utilization and evaluation of coalfield fire applying heat pipe combined thermoelectric generator in Xinjiang, China, Energy 207 (2020) 118303, http://dx.doi.org/10.1016/j.energy.2020.118303.
[15] Y. Zhao, Y. Fan, W. Li, Y. Li, M. Ge, L. Xie, Experimental investigation of heat pipe thermoelectric generator, Energy Convers. Manage. 252 (2022) 115123, http://dx.doi.org/10.1016/j.enconman.2021.115123.
[16] L. Catalan, P. Aranguren, M. Araiz, G. Perez, D. Astrain, New opportunities for electricity generation in shallow hot dry rock fields: A study of thermoelectric generators with different heat exchangers, Energy Convers. Manage. 200 (2019) 112061, http://dx.doi.org/10.1016/j.enconman.2019.112061.
[17] L. Catalan, M. Araiz, P. Aranguren, D. Astrain, Computational study of geothermal thermoelectric generators with phase change heat exchangers, Energy Convers. Manage. 221 (2020) 113120, http://dx.doi.org/10.1016/j.enconman.2020.113120.
[18] P. Alegria, L. Catalan, M. Araiz, A. Rodriguez, D. Astrain, Experimental development of a novel thermoelectric generator without moving parts to harness shallow hot dry rock fields, Appl. Therm. Eng. 200 (2022) 117619, http://dx.doi.org/10.1016/j.applthermaleng.2021.117619.
[19] L. Catalan, M. Araiz, P. Aranguren, G.D. Padilla, P.A. Hernandez, N.M. Perez, C. Garcia de la Noceda, J.F. Albert, D. Astrain, Prospects of autonomous volcanic monitoring stations : Experimental investigation on thermoelectric generation from fumaroles, Sensors 20 (2020) 3547, http://dx.doi.org/10.3390/s20123547.
[20] L. Catalan, A. Garacochea, A. Casi, M. Araiz, P. Aranguren, D. Astrain, Experimental evidence of the viability of thermoelectric generators to power volcanic monitoring stations, Sensors 20 (2020) 4839, http://dx.doi.org/10.3390/s20174839.
[21] Y. Huang, W. Li, D. Xu, Y. Wu, Spatiotemporal rule of heat transfer on a soil/finned tube interface, Sensors 19 (2019) 1159, http://dx.doi.org/10.3390/s19051159.
[22] K. Li, G. Garrison, M. Moore, Y. Zhu, C. Liu, R. Horne, S. Petty, An expandable thermoelectric power generator and the experimental studies on power output, Int. J. Heat Mass Transfer 160 (2020) 120205, http://dx.doi.org/10.1016/j.ijheatmasstransfer.2020.120205.
[23] C. Liu, P. Chen, K. Li, A 500 W low-temperature thermoelectric generator: Design and experimental study, Int. J. Hydrogen Energy 39 (2014) 15497–15505, http://dx.doi.org/10.1016/j.ijhydene.2014.07.163.
[24] C. Liu, P. Chen, K. Li, A 1 KW Thermoelectric Generator for Low-temperature Geothermal Resources, in: Thirty-Ninth Workshop on Geothermal Reservoir Engineering, 2014, pp. 1–12.
[25] J. Chen, K. Li, C. Liu, M. Li, Y. Lv, L. Jia, S. Jiang, Enhanced efficiency of thermoelectric generator by optimizing mechanical and electrical structures, Energies 10 (2017) 1329, http://dx.doi.org/10.3390/en10091329.
[26] K. Li, G. Garrison, Y. Zhu, M. Moore, C. Liu, J. Hepper, L. Bandt, R. Horne, S. Petty, Thermoelectric power generator: Field test at bottle rock geothermal power plant, J. Power Sources 485 (2021) 229266, http://dx.doi.org/10.1016/j.jpowsour.2020.229266.
[27] J. Diez-Gil, V. Araña, R. Ortiz, J. Yuguero, Stationary convection model for heat transfer by means of geothermal fluids in post eruptive systems, Geothermics 16 (1987) 77–89.

[28] Adafruit, Thermocouple Amplifier MAX31855 breakout board, 2020, URL https://www.adafruit.com/product/269.
[29] Adafruit, INA219 High Side DC Currect Sensor Breakout, 2020, URL https://www.adafruit.com/product/904.
[30] MeteoBlue, Clima lanzarote, 2022, URL https://www.meteoblue.com/es/tiempo/historyclimate/climatemodelled/lanzarote_espa~na_2515699.
[31] II.-V.I. Marlow Industries, TG12-8-01LS, 2020, URL https://ii-vi.com/product/thermoelectric-generator-teg-modules/.